Technical Note

High-Resolution Real-Time Spiral MRI for Guiding Vascular Interventions in a Rabbit Model at 1.5T

Masahiro Terashima, MD, PhD,[1] MinSu Hyon, MD,[1] Erasmo de la Pena-Almaguer, MD,[1] Phillip C. Yang, MD,[1] Bob S. Hu, MD,[2] Krishna S. Nayak, PhD,[3] John M. Pauly, PhD,[2] and Michael V. McConnell, MD, MSEE[1,2]*

Purpose: To study the feasibility of a combined high spatial and temporal resolution real-time spiral MRI sequence for guiding coronary-sized vascular interventions.

Materials and Methods: Eight New Zealand White rabbits (four normal and four with a surgically-created stenosis in the abdominal aorta) were studied. A real-time interactive spiral MRI sequence combining 1.1 × 1.1 mm^2 in-plane resolution and 189-msec total image acquisition time was used to image all phases of an interventional procedure (i.e., guidewire placement, balloon angioplasty, and stenting) in the rabbit aorta using coronary-sized devices on a 1.5 T MRI system.

Results: Real-time spiral MRI identified all rabbit aortic stenoses and provided high-temporal-resolution visualization of guidewires crossing the stenoses in all animals. Angioplasty balloon dilatation and deployment of coronary-sized copper stents in the rabbit aorta were also successfully imaged by real-time spiral MRI.

Conclusion: Combining high spatial and temporal resolution with spiral MRI allows real-time MR-guided vascular intervention using coronary-sized devices in a rabbit model. This is a promising approach for guiding coronary interventions.

Key Words: interventional MRI; real-time MRI; spiral MRI; vascular disease; MR angiography
J. Magn. Reson. Imaging 2005;22:687–690.

MAGNETIC RESONANCE IMAGING (MRI) guidance of interventional procedures offers several advantages over x-ray fluoroscopy. MRI is not limited to projection imaging and provides excellent soft-tissue contrast, which allows imaging of the vessel lumen, the vessel wall, and the surrounding tissue. Also, MRI does not involve the use of iodinated contrast material or ionizing radiation. However, MRI has the primary disadvantage of providing lower spatial and temporal resolution (e.g., 0.5–0.7 mm over 14 heartbeats for coronary MRA (1–3)) compared to x-ray fluoroscopy (0.2 mm, 30+ frames per second (fps)).

In previous studies, MRI guidance has been applied to a variety of cardiovascular interventions, including diagnostic cardiac catheterization for congenital heart disease (4,5), intracardiac device placement (6), intramyocardial therapy (7,8), and coronary and vascular interventions (9–12). While these studies demonstrated the feasibility of MRI guidance, the choice of the MRI sequence typically required a compromise between spatial and temporal resolution. High temporal resolution requires low spatial resolution or projection imaging, while high spatial resolution requires long acquisition times to acquire a complete image.

Spiral MRI techniques provide a highly efficient means of acquiring k-space data (2). As such, spiral MRI has advantages for both spatial and temporal resolution. In this study we implemented a combined high spatial and temporal resolution, real-time spiral MRI sequence and tested the feasibility of MRI guidance for coronary-sized vascular interventions. Specifically, we studied multiple steps of a real-time spiral MRI-guided vascular intervention using coronary-sized devices in the rabbit aorta model at 1.5T.

MATERIALS AND METHODS

MRI Techniques

All imaging studies were performed on a 1.5 T GE Signa scanner (GE Healthcare, Milwaukee, WI, USA) equipped with high-performance gradients (40 mT/m amplitude, 150 mT/m/msec slew rate). The body coil was used for RF transmission and a standard GE single-channel transmit/receive extremity coil was used for signal reception. A real-time interactive workstation (Sun Microsystems, Mountain View, CA, USA) located

[1]Division of Cardiovascular Medicine, Stanford University School of Medicine, Stanford, California, USA.
[2]Magnetic Resonance Systems Research Laboratory, Department of Electrical Engineering, Stanford University, Stanford, California, USA.
[3]Department of Electrical Engineering, University of Southern California, Los Angeles, California, USA.
*Address reprint requests to: M.V.M., Division of Cardiovascular Medicine, Stanford University School of Medicine, Room H-2157, 300 Pasteur Drive, Stanford, CA 94305-5233.
E-mail: mcconnell@stanford.edu

Contract grant sponsor: National Institutes of Health; Contract grant numbers: R01-EB002992; R01-HL39297; Contract grant sponsors: GE Healthcare; Donald W. Reynolds Cardiovascular Clinical Research Center, Stanford University.

The Supplementary Material referred to in this article can be accessed at http://www.interscience.wiley.com/jpages/1053-1807/suppmat/index.html.

Received November 15, 2004; Accepted June 15, 2005.

DOI 10.1002/jmri.20409
Published online 10 October 2005 in Wiley InterScience (www.interscience.wiley.com).

adjacent to the scanner console was used to run the spiral sequences, perform real-time image reconstruction and display, and store images (3).

The high-resolution, real-time spiral MRI sequence we developed consisted of an interleaved spiral acquisition (FOV = 20 cm, slice thickness = 5 mm, flip angle = 30°, seven interleaves, TR = 27 msec, TE = 4.6 msec), and achieved an in-plane spatial resolution of 1.1×1.1 mm^2 (13). Full image acquisition required 189 msec (TR = 27 msec per interleaf $\times$ 7 interleaves). With a sliding window reconstruction (14), images could be updated and displayed in real-time with each new interleaf (i.e., 1/7 of the data replaced every 27 msec). This allowed imaging up to 37 fps, and was typically viewed at 16–20 fps. At 20 fps, images were displayed approximately every 2 TR (or 54 msec), with 2/7 of the data replaced with each image update.

Multislice (non-real-time) spiral MRA was also performed at each stage of the interventional procedure to further confirm device location/placement and procedure outcome (see description of the workflow below). This provided even higher spatial resolution (0.4×0.4 mm^2) using a sequence designed for coronary MRA (TR = 1000 msec, TE = 4.6 msec, FOV = 16 cm, slice thickness = 3.0 mm, flip angle = 60°, five slices, acquisition time = 40 seconds) (1–3).

Animal Model

We studied eight New Zealand White rabbits (weight 3.0–3.5 kg): four normal (non-operated) and four with a surgically created stenosis in the abdominal aorta (15), which is similar in size to the human coronary artery (3–4 mm diameter). The experimental protocol was approved by the administrative panel on laboratory animal care of our institution. Anesthesia was induced by injection of glycopyrrolate (0.02 mg/kg, subcutaneously), medetomidine (350 mg/kg, intramuscularly), and ketamine (40 mg/kg, intramuscularly). The rabbits were intubated and anesthesia was maintained with 3.0% halothane and oxygen. Following a midline abdominal incision, a 3-cm-long segment of the abdominal aorta was exposed. The exposed aortic portion (suprarenal in three, and infrarenal in one) was wrapped tightly with a 5-mm-wide Dacron band and the abdominal incision was closed.

Interventional Procedure and Workflow

In the rabbits with surgically created aortic stenoses, MRI was performed one month after surgery. Since the stenosis was surgically created and resistant to dilation, stent deployment was not tested in these animals. The animals were sedated for the MR study with ketamine (35 mg/kg) and xylazine (5 mg/kg) intramuscularly. A 5 Fr introducer sheath (7.5 cm long; Arrow International Inc., Reading, PA, USA) was inserted via the right femoral artery. Both stainless steel (0.014 inch in diameter; Guidant Corp., Santa Clara, CA, USA) and low-artifact nitinol with hydrophilic coating (0.018–0.035 inch in diameter; Terumo Corp., Tokyo, Japan) guidewires were tested. After the guidewire was placed in the aorta, a standard coronary angioplasty balloon (20 mm $\times$ 4.0 mm; ACS RX COMET, Guidant Corp.) was advanced into the aorta. This angioplasty balloon was selected because it had platinum-iridium markers at the proximal and distal ends of the balloon, which generate minimal MR artifacts. The angioplasty balloon was inflated up to 12 atm and maintained for 20 seconds with a standard balloon inflation device (20 mL, 20 atm; Guidant Corp.) filled with diluted gadopentetate dimeglumine (1:300, 1.6 mg/mL; Magnevist; Berlex Laboratories, Wayne, NJ, USA) to visualize the inflating balloon. In two animals a coronary-sized copper stent (3.5 $\times$ 6.0 mm; Pulse Medical Systems, Collegeville, PA, USA) was mounted on the balloon and deployed in the aorta. Copper stents were used because they have been shown to have minimal MR artifacts (16). All animals were euthanized after the entire interventional procedure was completed and examined for evidence of complications in the aorta, such as vessel rupture or occlusion.

To perform the MRI-guided interventions, one operator ran the real-time workstation adjacent to the console from outside the scan room, while another performed the interventional procedures in the scan room, coordinated by visual and verbal communication. The workflow was as follows: 1) the real-time spiral MRI sequence (RT) was run first to localize the abdominal aorta and stenosis, 2) a baseline multislice (non-real-time) spiral MRA acquisition (MRA) of the aorta and stenosis was performed, 3) RT was performed during the active intervention (i.e., device advancement, balloon inflation, stent deployment, etc.), 4) MRA was performed to further confirm device position/deployment, and 5) both RT and MRA were performed postprocedure to image the results and detect any procedural complications (e.g., vessel rupture, occlusion).

RESULTS

The real-time spiral MRI sequence allowed successful imaging of the entire abdominal aorta and important landmarks (renal arteries and iliac arteries) in all of the rabbits. In the diseased rabbits, all aortic stenoses and nearby landmarks of the renal arteries were visualized using real-time spiral MRI.

Standard stainless steel guidewires generated large artifacts, which were substantially greater than the size of the abdominal aorta. Nitinol guidewires caused much smaller artifacts, and allowed passive visualization of the guidewire (including the tip) as well as the vessel anatomy. Real-time spiral MRI was able to guide the passage of nitinol guidewires in the aorta, including successful passing across all the stenoses. The most instructive case involved a tight stenosis that did not allow passage of a 0.035-inch guidewire (Fig. 1). Real-time spiral MRI provided rapid image feedback that the vessel was being torqued on one attempt (Fig. 1b) and that the tip looped back down the aorta (Fig. 1c) on another attempt. The wire was changed to 0.018 inch, which crossed successfully.

Next, the angioplasty balloon was placed using real-time spiral MRI guidance (as shown in Fig. 2). The platinum-iridium markers in the balloon allowed visualization of the balloon straddling the stenoses. The

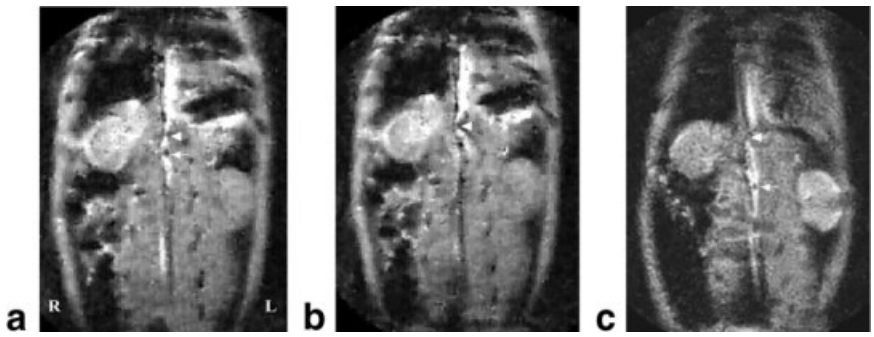

Figure 1. Real-time spiral MRI of guidewire crossing attempts. **a:** The tip (arrow) of the 0.035-inch nitinol guidewire is seen just below the stenosis (arrowhead) in the rabbit aorta. **b:** As the guidewire meets resistance when advanced, one can see that the vessel is distorted at the site of the stenosis (arrowhead). Supplementary Material for this article can be found at http://www.interscience.wiley.com/jpages/1053-1807/suppmat/index.html. **c:** On another attempt, the tip of the guidewire (arrow) is seen looping back down the aorta.

entire length of the gadolinium-filled balloon during inflation was imaged under real-time spiral MRI. Multislice spiral MRA performed pre- and post-dilatation revealed no complications (e.g., rupture of the aorta), which was confirmed by postmortem evaluation. Since the stenosis was surgically sutured, we did not expect (nor detect) any significant change in the degree of stenosis.

Finally, real-time spiral MRI successfully imaged stent deployment (Fig. 2). With the minimal artifact of the copper stent, the platinum-iridium markers of the balloon again allowed visualization of device position within the aorta (Fig. 2a). Furthermore, the gadolinium-filled balloon within the stent was clearly visualized by real-time spiral MRI during the entire balloon inflation (Fig. 2b). Post-stent multislice spiral MRA showed successful deployment without complications (Fig 2b inset), which was also confirmed postmortem.

DISCUSSION

In this study, we have demonstrated the feasibility of a combined high spatial and temporal resolution, real-time spiral MRI sequence to guide multiple steps of a vascular intervention using coronary-sized devices in a rabbit model. Our real-time spiral MRI sequence had adequate spatial resolution to image these small vessels and devices while it also provided rapid image feedback of device manipulation and effect.

For MRI-guided cardiovascular interventions, especially coronary interventions, it would be ideal to combine the high spatial and temporal resolution of x-ray with the tissue imaging capabilities of MRI. It is challenging to visualize small devices, as well as small and rapidly moving coronary arteries, by MRI. Nonetheless, many successful studies of MR-guided vascular interventions have been performed. One approach is to acquire high-resolution, non-real-time "roadmap" images and then use real-time projection imaging of active devices to overlay on the roadmap (17). Alternatively, studies have used lower spatial resolution, real-time MRI applied to larger vessels, such as the pulmonary artery (18), abdominal aorta (19,20), iliac (11,21), and renal artery (22,23) in pigs. A recent study also used real-time spiral MRI for larger pig abdominal aortae (20–30 mm diameter) (20), albeit with more limited temporal (309 msec, 10 fps) and spatial resolution (1.3 mm). Alternative promising approaches include real-

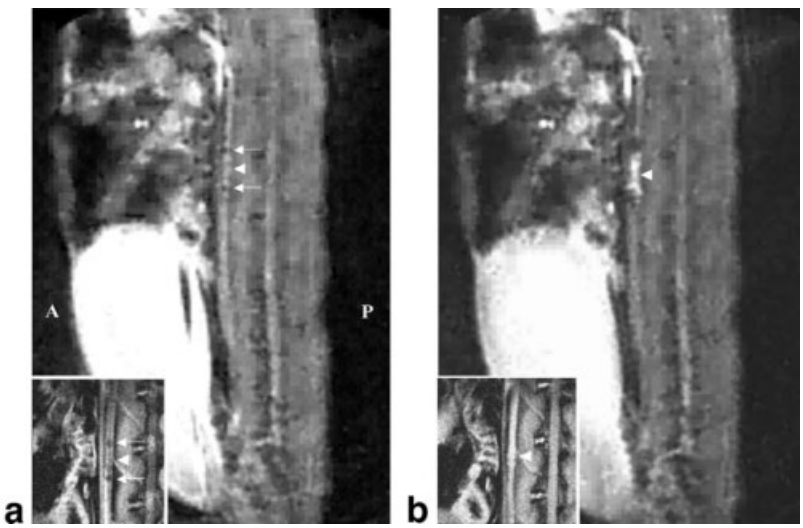

Figure 2. MRI guidance of balloon dilatation and stenting. **a:** Sagittal real-time spiral MRI and multislice spiral MRA (inset) show the uninflated angioplasty balloon markers (arrows), with the copper stent located between (arrowhead), in the rabbit aorta. **b:** Real-time spiral MRI shows the length of the inflated gadolinium-filled angioplasty balloon (arrowhead) deploying the stent. High-resolution multislice spiral MRA (inset) confirmed the intact, mildly dilated aorta at the stent site (arrowhead). Supplementary Material for this article can be found at http://www.interscience.wiley.com/jpages/1053-1807/suppmat/index.html.

time radial MRI (11) and real-time steady-state free precession (SSFP) (10). While radial MRI can achieve high spatial resolution (1.2×1.2 mm^2) with high frame rates (e.g., 20 fps using sliding-window reconstruction), the full image acquisition duration is over three seconds since over 300 radials are needed per image. Thus, at 20 fps and a TR of 12 msec, each new frame contains only four to five new radials or <2% new data. Our spiral real-time MRI sequence is approximately 19-fold faster (full image acquisition duration of 189 msec), which results in >25% new data when reconstructed at 20 fps. Real-time radial SSFP (10) has SNR advantages and can acquire a full image in 200 msec, similarly to our method, but with a significant reduction (more than twofold) in spatial resolution (2.3 mm vs. 1.1 mm).

Since the primary focus of this study was to evaluate the high spatial/temporal resolution real-time spiral MRI sequence, we used passive tracking of primarily off-the-shelf coronary devices. Device visualization may be further enhanced by using active catheter coils (17). Importantly, our ability to track the devices passively in real time was aided by our ability to rapidly follow the motion of the devices in combination with high spatial resolution to see the guidewire tip and angioplasty balloon markers.

A significant limitation is that we studied the rabbit aorta as a model for a coronary-sized vessel rather than a coronary artery. Furthermore, we used a rigid, nonatherosclerotic model of vascular stenosis, which limits assessment of therapeutic interventions. Clearly, these spiral real-time sequences must be tested in more human-like coronary stenoses in large animals (e.g., pig) before translation to humans is considered. A further improvement would be to place the workstation control/display in the scan room. Finally, although we did not see any gross pathologic evidence of vessel damage, a more detailed assessment of device heating and safety would also be required prior to human use.

In conclusion, we have demonstrated success using a combined high spatial and temporal resolution, real-time spiral MRI sequence for real-time MRI guidance of coronary-sized vascular interventions. This is a promising approach for combining the spatial/temporal resolution needed for device guidance with the tissue imaging capabilities of MRI to improve cardiovascular interventional procedures.

ACKNOWLEDGMENTS

The authors thank Dr. Chengpei Xu for surgical instruction, and Dr. Phillip Tsao for advice on the animal model.

REFERENCES

1. Terashima M, Meyer CH, Keeffe BG, et al. Noninvasive assessment of coronary vasodilation using magnetic resonance angiography. J Am Coll Cardiol 2005;45:104–110.
2. Meyer CH, Hu BS, Nishimura DG, Macovski A. Fast spiral coronary artery imaging. Magn Reson Med 1992;28:202–213.
3. Yang PC, Meyer CH, Terashima M, et al. Spiral magnetic resonance coronary angiography with rapid real-time localization. J Am Coll Cardiol 2003;41:1134–1141.
4. Razavi R, Hill DL, Keevil SF, et al. Cardiac catheterisation guided by MRI in children and adults with congenital heart disease. Lancet 2003;362:1877–1882.
5. Schalla S, Saeed M, Higgins CB, Martin A, Weber O, Moore P. Magnetic resonance—guided cardiac catheterization in a swine model of atrial septal defect. Circulation 2003;108:1865–1870.
6. Rickers C, Jerosch-Herold M, Hu X, et al. Magnetic resonance image-guided transcatheter closure of atrial septal defects. Circulation 2003;107:132–138.
7. Lederman RJ, Guttman MA, Peters DC, et al. Catheter-based endomyocardial injection with real-time magnetic resonance imaging. Circulation 2002;105:1282–1284.
8. Susil RC, Yeung CJ, Halperin HR, Lardo AC, Atalar E. Multifunctional interventional devices for MRI: a combined electrophysiology/MRI catheter. Magn Reson Med 2002;47:594–600.
9. Serfaty JM, Yang X, Foo TK, Kumar A, Derbyshire A, Atalar E. MRI-guided coronary catheterization and PTCA: a feasibility study on a dog model. Magn Reson Med 2003;49:258–263.
10. Spuentrup E, Ruebben A, Schaeffter T, Manning WJ, Gunther RW, Buecker A. Magnetic resonance-guided coronary artery stent placement in a swine model. Circulation 2002;105:874–879.
11. Buecker A, Adam GB, Neuerburg JM, et al. Simultaneous real-time visualization of the catheter tip and vascular anatomy for MR-guided PTA of iliac arteries in an animal model. J Magn Reson Imaging 2002;16:201–208.
12. Omary RA, Green JD, Schirf BE, Li Y, Finn JP, Li D. Real-time magnetic resonance imaging-guided coronary catheterization in swine. Circulation 2003;107:2656–2659.
13. Nayak KS, Pauly JM, Yang PC, Hu BS, Meyer CH, Nishimura DG. Real-time interactive coronary MRA. Magn Reson Med 2001;46:430–435.
14. Riederer SJ, Tasciyan T, Farzaneh F, Lee JN, Wright RC, Herfkens RJ. MR fluoroscopy: technical feasibility. Magn Reson Med 1988;8:1–15.
15. Xu C, Zarins CK, Pannaraj PS, Bassiouny HS, Glagov S. Hypercholesterolemia superimposed by experimental hypertension induces differential distribution of collagen and elastin. Arterioscler Thromb Vasc Biol 2000;20:2566–2572.
16. Buecker A, Spuentrup E, Ruebben A, Gunther RW. Artifact-free in-stent lumen visualization by standard magnetic resonance angiography using a new metallic magnetic resonance imaging stent. Circulation 2002;105:1772–1775.
17. Yang X, Atalar E. Intravascular MR imaging-guided balloon angioplasty with an MR imaging guide wire: feasibility study in rabbits. Radiology 2000;217:501–506.
18. Kuehne T, Saeed M, Higgins CB, et al. Endovascular stents in pulmonary valve and artery in swine: feasibility study of MR imaging-guided deployment and postinterventional assessment. Radiology 2003;226:475–481.
19. Godart F, Beregi JP, Nicol L, et al. MR-guided balloon angioplasty of stenosed aorta: in vivo evaluation using near-standard instruments and a passive tracking technique. J Magn Reson Imaging 2000;12:639–644.
20. Mahnken AH, Chalabi K, Jalali F, Gunther RW, Buecker A. Magnetic resonance-guided placement of aortic stents grafts: feasibility with real-time magnetic resonance fluoroscopy. J Vasc Interv Radiol 2004;15:189–195.
21. Dion YM, Ben El Kadi H, Boudoux C, et al. Endovascular procedures under near-real-time magnetic resonance imaging guidance: an experimental feasibility study. J Vasc Surg 2000;32:1006–1014.
22. Omary RA, Frayne R, Unal O, et al. MR-guided angioplasty of renal artery stenosis in a pig model: a feasibility study. J Vasc Interv Radiol 2000;11:373–381.
23. Wacker FK, Reither K, Ebert W, Wendt M, Lewin JS, Wolf KJ. MR image-guided endovascular procedures with the ultrasmall superparamagnetic iron oxide SH U 555 C as an intravascular contrast agent: study in pigs. Radiology 2003;226:459–464.